



Platform

# SunCHECK<sup>®</sup>

## One Database for Complete Quality Management

[Learn more >](#)



Patient

- Plan Quality Checks
- Secondary Dose Calculations
- Pre-Treatment QA
- In-Vivo Monitoring



Machine

- Standardized Routine QA
- Direct Device Control
- Automated Imaging, MLC & VMAT QA
- Protocol-Based QA



# Calibration method and performance of a time-of-flight detector to measure absolute beam energy in proton therapy

Anna Vignati<sup>1,2</sup> | Felix Mas Milian<sup>1,2,3</sup> | Zahra Shakarami<sup>1,2</sup> |  
 Mohammed Abujami<sup>1,2</sup> | Davide Bersani<sup>1,2</sup> | Emanuele Data<sup>1,2</sup> | Marco Donetti<sup>4</sup> |  
 Veronica Ferrero<sup>2</sup> | Cosimo Galeone<sup>1,2</sup> | Simona Giordanengo<sup>2</sup> |  
 Omar Hammad Ali<sup>5</sup> | Oscar Ariel Marti Villarreal<sup>1,2</sup> | Elisabetta Medina<sup>1,2</sup> |  
 Diango Montalvan Olivares<sup>1,2</sup> | Giovanni Paternoster<sup>5</sup> | Francesco Tommasino<sup>6,7</sup> |  
 Roberto Cirio<sup>1,2</sup> | Vincenzo Monaco<sup>1,2</sup> | Roberto Sacchi<sup>1,2</sup>

<sup>1</sup>Dipartimento di Fisica, Università degli Studi di Torino, Torino, Italy

<sup>2</sup>INFN, sezione di Torino, Torino, Italy

<sup>3</sup>Department of Exact and Technological Sciences, Universidade Estadual de Santa Cruz, Ilhéus, Brazil

<sup>4</sup>Centro Nazionale di Adroterapia Oncologica, CNAO, Pavia, Italy

<sup>5</sup>FBK, Fondazione Bruno Kessler, Center for Sensors and Devices, Trento, Italy

<sup>6</sup>Trento Institute for Fundamental Physics and Applications, TIFPA-INFN, Povo, Trento, Italy

<sup>7</sup>Department of Physics, University of Trento, Povo, Trento, Italy

## Correspondence

Felix Mas Milian, Dipartimento di Fisica, Università degli Studi di Torino, INFN, sezione di Torino, Torino, Italy.  
 Email: [felix.masmilian@unito.it](mailto:felix.masmilian@unito.it)

## Funding information

MIUR Dipartimenti di Eccellenza 2018-2022, Italy; 5th Scientific Commission (CSN), INFN, Italy; MIUR PRIN 2017, Grant/Award Number: 2017L2XKTJ

## Abstract

**Background:** The beam energy is one of the most significant parameters in particle therapy since it is directly correlated to the particles' penetration depth inside the patient. Nowadays, the range accuracy is guaranteed by offline routine quality control checks mainly performed with water phantoms, 2D detectors with PMMA wedges, or multi-layer ionization chambers. The latter feature low sensitivity, slow collection time, and response dependent on external parameters, which represent limiting factors for the quality controls of beams delivered with fast energy switching modalities, as foreseen in future treatments. In this context, a device based on solid-state detectors technology, able to perform a direct and absolute beam energy measurement, is proposed as a viable alternative for quality assurance measurements and beam commissioning, paving the way for online range monitoring and treatment verification.

**Purpose:** This work follows the proof of concept of an energy monitoring system for clinical proton beams, based on Ultra Fast Silicon Detectors (featuring tenths of ps time resolution in 50  $\mu\text{m}$  active thickness, and single particle detection capability) and time-of-flight techniques. An upgrade of such a system is presented here, together with the description of a dedicated self-calibration method, proving that this second prototype is able to assess the mean particles energy of a monoenergetic beam without any constraint on the beam temporal structure, neither any a priori knowledge of the beam energy for the calibration of the system.

**Methods:** A new detector geometry, consisting of sensors segmented in strips, has been designed and implemented in order to enhance the statistics of coincident protons, thus improving the accuracy of the measured time differences. The prototype was tested on the cyclotron proton beam of the Trento Protontherapy Center (TPC). In addition, a dedicated self-calibration method, exploiting the measurement of monoenergetic beams crossing the two telescope sensors for

Anna Vignati, Felix Mas Milian, and Zahra Shakarami contributed equally to this work and share first authorship.

This is an open access article under the terms of the [Creative Commons Attribution](https://creativecommons.org/licenses/by/4.0/) License, which permits use, distribution and reproduction in any medium, provided the original work is properly cited.

© 2023 The Authors. *Medical Physics* published by Wiley Periodicals LLC on behalf of American Association of Physicists in Medicine.

different flight distances, was introduced to remove the systematic uncertainties independently from any external reference.

**Results:** The novel calibration strategy was applied to the experimental data collected at TPC (Trento) and CNAO (Pavia). Deviations between measured and reference beam energies in the order of a few hundreds of keV with a maximum uncertainty of 0.5 MeV were found, in compliance with the clinically required water range accuracy of 1 mm.

**Conclusions:** The presented version of the telescope system, minimally perturbative of the beam, relies on a few seconds of acquisition time to achieve the required clinical accuracy and therefore represents a feasible solution for beam commission, quality assurance checks, and online beam energy monitoring.

#### KEYWORDS

energy measurement, proton therapy, silicon sensor

## 1 | INTRODUCTION

The longitudinal penetration depth of beams used to treat patients in particle therapy (PT) depends on their energy, and it is therefore considered one of the critical irradiation parameters.<sup>1</sup>

Nowadays, a great effort of the PT research community is focused on developing new accelerating and delivery systems allowing for quick changes of the beam energy, as this could improve the treatment time, especially for gating and rescanning modalities, and foster the treatment of moving targets by providing fast range adaptation for implementing 4D spot scanning treatment.<sup>1,2</sup>

However, such developments imply, in parallel, the introduction of a fast and precise beam energy control in the beam monitoring system, which could be exploited both for regular quality assurance (QA) procedures and for providing full control of the primary beam during irradiation.

At present, existing detectors<sup>3</sup> do not measure the beam energy during treatment and the proper accuracy of the extracted beam energy is guaranteed by the safe checks of accelerator settings, by an advanced beam diagnostics and interlock system which guarantee the correct beam orbit through the beam transport elements and daily QA measurements of the penetration depth.<sup>4-7</sup>

The proof of concept of a telescope of two Ultra Fast Silicon Detectors (UFSD), able to directly measure the proton beam energy and meeting the clinically required accuracy, corresponding to a maximum error of 1 mm particle range in water, has been recently demonstrated.<sup>8-11</sup> The proposed detector assesses the mean energy of clinical proton beams by measuring the protons' Time of Flight (ToF), that is, the time needed by single protons to travel a known distance between two sensors. The ToF is a well-known technique that found several applications in the last decades,<sup>11</sup> from nuclear physics<sup>12</sup> to proton radiography,<sup>13-15</sup> from the measurement of the kinetic energy of cyclotron

and LINAC proton beams up to 30 MeV,<sup>16,17</sup> to the reconstruction of the proton energy spectrum of high-energy laser-driven beams.<sup>18</sup>

The first system prototype proposed by the University and the National Institute for Nuclear Physics (INFN) of Turin, Italy, and its test on clinical beams are described in detail in previous work,<sup>11</sup> and will be rapidly summarized in the following. The first telescope was made of two 80  $\mu\text{m}$  thick UFSD sensors. It was tested at Centro Nazionale Adroterapia Oncologica (CNAO, Pavia, Italy) at clinical proton energies (from 60 up to 230 MeV) with fluxes at the lower limit of the ones typically used in clinics ( $10^8 \text{ p s}^{-1} \text{ cm}^{-2}$ ). During the test using a ToF system not optimized in efficiency, 6 s (corresponding to  $\sim 2$  ms active acquisition time) of irradiation were necessary to keep the ToF statistical error below 3 ps at 1 m distance between the sensors. As shown in a previous article,<sup>11</sup> 3 ps correspond to the tolerance mentioned above of 1 mm range in water for 230 MeV protons. Following the published promising results, several improvements of the first system prototype have been undertaken: a new sensor geometry has been designed and produced specifically to enlarge the sensitive area and, consequently, enrich the statistics collection of coincident proton signals; a dedicated mechanical support has been developed to vary the distance between the sensors in a controlled way.

The second version of the telescope system, made of two UFSD sensors segmented in strips, was tested at the Trento Protontherapy Center (TPC),<sup>19</sup> on a proton beam structure different from the CNAO one considered for the tests of the first telescope prototype.<sup>11</sup> More specifically, at the TPC, protons are delivered in synchronous with the cyclotron radiofrequency of 106 MHz (9.4 ns period), and the beam current is modulated by a 50% duty cycle square wave with a 100 ms period,<sup>19</sup> resulting in the bunched structure of the beam, different from the CNAO quasi-uniform one. Therefore, the present work aims at showing that the excellent time resolution and very short signals ( $\sim 2$  ns) provided by the UFSD technology allow for determining the beam

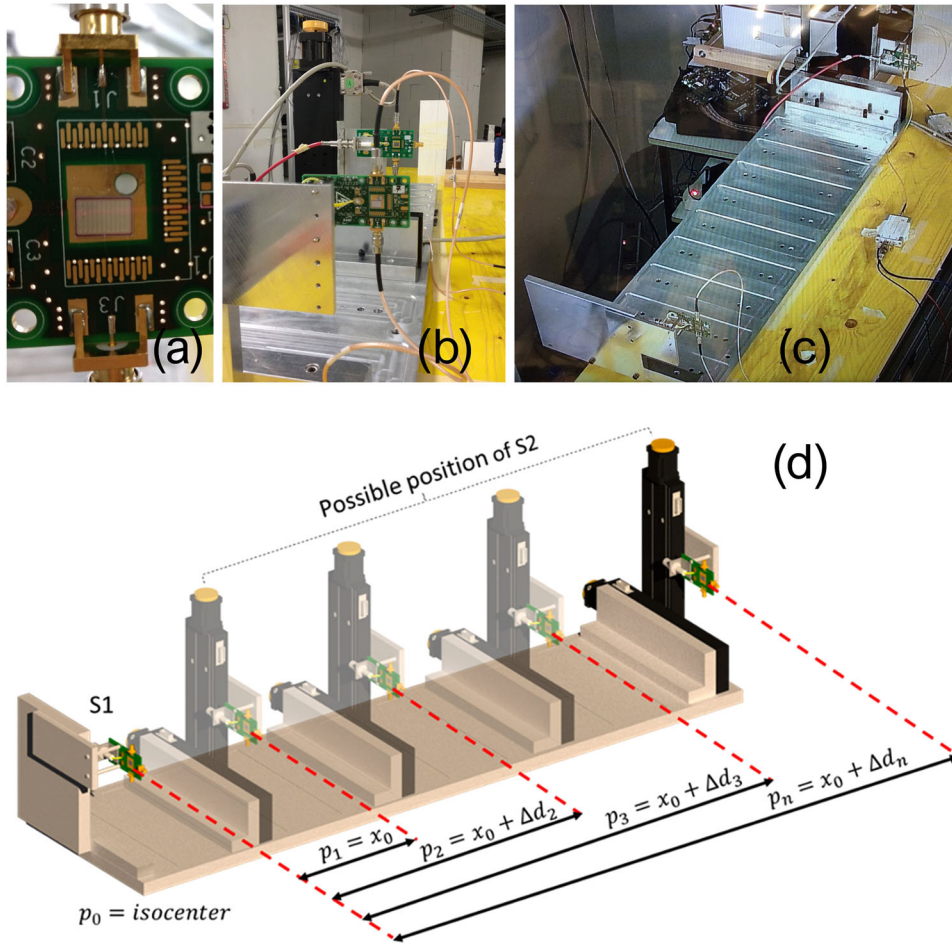


**FIGURE 1** (a) FBK sensor segmented in 11 strips (only one channel was connected to the signal output connector). (b) Telescope with the two channels general purpose high voltage (HV) distribution boards used to readout the sensor. (c) CCTV image of the setup at the TPC control room. (d) Schematic view of the mechanical support for positioning of sensor 2 (S2) at 10 different relative positions from sensor 1 (S1), which is kept fixed at the isocenter of the irradiation facility.

energy without any constraint on the beam temporal structure and with minimal perturbation of the particle trajectory. Moreover, a self-calibration approach, independent from any a priori knowledge of the beam energy, is here described, able to experimentally determine the systematic errors depending on the setup, such as the distance between the sensors and the time delays between channels originating from the routing of the electronic chain. The self-calibration method has been applied to the experimental data collected at TPC and CNAO. A comparison with the first calibration approach presented in a previous paper<sup>11</sup> is also reported.

## 2 | MATERIALS AND METHODS

### 2.1 | Telescope system of two UFSD strip sensors and readout electronics

A telescope prototype for the ToF measurement was built using two UFSD sensors (named S1 and S2, hereinafter), placed at a specific relative position between

each other and aligned along the beam direction (Figure 1). Differently from the first published prototype, where 2 Hamamatsu Photonics K.K. pad sensors were used, dedicated sensors segmented in 11 strips (10 with gain and 1 without gain, Figure 1a), were manufactured by Fondazione Bruno Kessler (FBK, Trento, Italy) using both Epitaxial and Si-Si wafers with a total thickness of 615/630  $\mu\text{m}$  and an active thickness of 45/55  $\mu\text{m}$ .<sup>20</sup> Furthermore, to minimize the beam perturbation, the passive silicon substrate was thinned down to reduce the total thickness crossed by each particle to 70  $\mu\text{m}$ . UFSD are n-in-p silicon sensors based on the low gain avalanche diode (LGAD) technology, featuring a moderate internal gain due to a thin p+ additional layer located below the n++ electrode of a heavily doped junction.<sup>21,22</sup> Their enhanced signal with fast rising edge leads to time resolutions as small as 30 ps in 50  $\mu\text{m}$  active thickness.<sup>23</sup> Therefore, UFSD sensors are ideally suited for ToF purposes and guarantee, at the same time, a reduced perturbation of the beam, as the properly thinned down thickness reduces the multiple scattering effects.

UFSD sensors were mounted on general-purpose high voltage (HV) distribution boards (Figure 1b), allowing only one out of the 11 strips to be readout through the signal output connector mounted on the board. The HV was set independently on the two sensors via the board connected to an external power supply DT1470ET (CAEN S.p.A., Viareggio, Italy); sensors signals were amplified by a low-noise current amplifier (Broadband Amplifier 2 GHz, CIVIDEC, Wien, Austria) and acquired by a 16 + 1 channels digitizer desktop module DT5742 (CAEN S.p.A., Viareggio, Italy). The digitizer samples the signal at 5 GS s<sup>-1</sup>, with 1 ADC count corresponding to 0.24 mV, and for each trigger stores 1024 samples corresponding to a waveform of 204.8 ns duration. A PC, connected to the digitizer with an 80 MB s<sup>-1</sup> optical link, was used to control the acquisition, collect the waveforms, and produce an asynchronous software trigger when the previous event was stored. An acquisition efficiency of 0.4‰ results from the conversion time of the digitizer (110 μs) and the time needed to transmit and store the data (~500 μs). The mechanical system of the ToF telescope (Figure 1c,d) consists of a rigid horizontal support with 10 grooves, machined with high precision (estimated uncertainty 100 μm) at 10 cm distance from each other, for positioning of S2 at nine different relative positions  $p_i$  from S1, the latter being kept at a fixed position in the isocenter of the irradiation facility. The allowed distances between sensors, measured with an external ruler, are approximately in the range of 7–97 cm. In order to align the two sensors with the beam direction, two movable stages were used to support and remotely displace S2 in two orthogonal directions transversely to the beam.

## 2.2 | Detector requirement

The relation between the kinetic energy  $K$  and the ToF of protons passing through the telescope is given by:

$$ToF(K, d) = \frac{(K + E_0) \cdot d}{c \cdot \sqrt{(K + E_0)^2 - E_0^2}} \quad (1)$$

where  $E_0$  is the proton mass energy at rest,  $c$  is the speed of light, and  $d$  is the traveled distance, that is, the position of S2 relative to S1. Once the mean ToF value is measured, the beam kinetic energy can be calculated by inverting Equation (1), after correcting for the energy loss in the first detector and in the air.<sup>11</sup>

The required ToF precision of a beam energy detector for clinical applications is strictly related to the maximum acceptable tolerance in the range uncertainty, which at CNAO and TPC is defined as 1 mm in water. A range uncertainty of 1 mm corresponds to a required resolution of the energy measurement ranging from ~1 MeV

at 60 MeV to ~0.4 MeV at 230 MeV, and the related maximum uncertainty on the ToF, for a flight distance of 1 m between the sensors, ranges from 80 ps at 60 MeV to 3 ps at 230 MeV, and these limits are more stringent for reduced distances. The ToF approach relies on identifying coincident signals, that is, signals generated in the two sensors of the telescope by the same proton crossing both of them.<sup>11</sup>

The precision of the average ToF measurement depends on the proton beam flux, typically in the range 10<sup>8</sup>–10<sup>10</sup> p s<sup>-1</sup> cm<sup>-2</sup> for clinical application, on the system deadtime and efficiency, and the duration of the beam irradiation; all these quantities influence the statistics of acquired coincident proton signals and the accuracy of the identification of the coincident signals over the combinatorial background.

The large dead time due to the abovementioned 0.4‰ acquisition efficiency currently represents the bottleneck for reducing the irradiation time needed to acquire sufficient statistics.

In addition, a good compromise between sensor size and travel distance must be chosen based on simulation studies, and a careful alignment system must be employed to maximize the number of coincidences and keep the combinatorial error at acceptable levels. The system efficiency, that is, the probability that a proton crossing the first sensor hits the second one at a specific distance along the beam trajectory, was addressed with Geant4.<sup>11</sup> The simulation results for different distances between sensors and different sensor areas demonstrated that a minimum size of 3 × 3 mm<sup>2</sup> is necessary for measurements at the largest distance to achieve a minimum efficiency of 10%. Similarly, the same simulations indicate that the beam interaction with 100-μm thick sensors increases the FWHM of the lateral proton profile by 3 mm in the worst case (60 MeV beam energy).

## 2.3 | ToF measurement and system calibration

Inverting Equation (1), the beam energy can be obtained from the ToF of protons, defined as:

$$ToF = \Delta t_{mean} - offset \quad (2)$$

where  $\Delta t_{mean}$  is the average value of the difference of proton crossing times measured in the two sensors and  $offset$  is a constant time difference mainly due to the routing of the electronic chain.

The identification of signals produced by coincident protons in the two sensors and the measurement of the corresponding  $\Delta t_{mean}$  is performed with the iterative statistical method described in a preceding publication.<sup>11</sup>

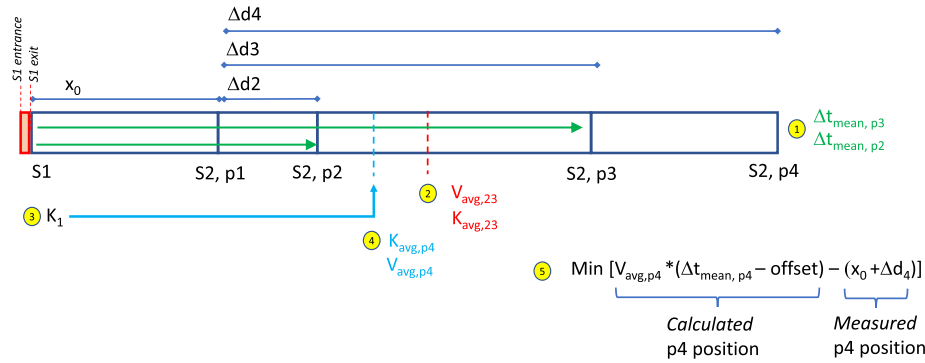


**FIGURE 2** Schematic of the self-calibration approach with subsequent steps in yellow. Step 1:  $\Delta t_{\text{mean}}$  is measured for two different S2 locations (p2 and p3 in the example); step 2: the average kinetic energy  $K_{\text{avg},23}$  between the two S2 locations (p2 and p3) is obtained; step 3: from  $K_{\text{avg},23}$ , the beam kinetic energy  $K_1$  at S1 exit is found; step 4: from  $K_1$  the average kinetic energy and average velocity for any traveled distance (p4 in the example) can be obtained; step 5: final minimization of the square deviation between calculated and measured S2 positions.

**TABLE 1** Self- (left column) and relative (right column) calibration parameters resulting from 16  $\Delta t_{\text{mean}}$  measurements (four energies and four distances) for the CNAO beam test.

| Self Parameter | Value | Error | Relative Parameter | Value  | Error |
|----------------|-------|-------|--------------------|--------|-------|
| offset (ps)    | 116.9 | 1.2   | offset (ps)        | 115.1  | 2.9   |
| $x_0$ (cm)     | 6.605 | 0.015 | $d_1$ (cm)         | 6.613  | 0.033 |
|                |       |       | $d_2$ (cm)         | 36.495 | 0.042 |
|                |       |       | $d_3$ (cm)         | 66.663 | 0.046 |
|                |       |       | $d_4$ (cm)         | 96.727 | 0.050 |

The main source of systematic errors resides in the uncertainty of the *offset* and the distance between the sensors, requiring a calibration procedure to determine their values. Two different calibration approaches will be described in the following, together with a comparison of the results obtained with both calibration methods on the data acquired in the first test at CNAO and the second at TPC.

### 2.3.1 | Reference energy values

The set of beam energy values at the isocenter used as a reference for our measurements were retrieved, using the PSTAR dataset of the National Institute of Standards and Technology, from the distal water equivalent depths measured as range 80% (R80) at CNAO and range 90% (R90) at TPC. At CNAO, the range measurements were performed using a Peakfinder (PTW, Freiburg, Germany) water column with a maximum deviation from the expected range within  $\pm 0.15$  mm,<sup>6</sup> whereas, at the TPC experimental facility, the Giraffe detector (IBA dosimetry, Louvain-la-Neuve, Belgium) was used featuring a larger uncertainty of  $\pm 0.5$  mm.<sup>19</sup> They were provided by the facility and hereinafter will be called *reference energies*.

### 2.3.2 | The relative approach

This calibration approach was adopted for calculating the beam energies from the data acquired at CNAO with the first prototype of the telescope system and relies on using the reference energies set.<sup>11</sup> Using the  $\Delta t_{\text{mean},ij}$  measured at different reference beam energies ( $K_i$ ) and by varying the distances  $d_j$  between the sensors, the system is calibrated through a  $\chi^2$  minimization:

$$\chi^2(\text{offset}, d_j) = \sum_{ij} \left\{ \frac{(\Delta t_{\text{mean},ij} - \text{offset}) - \text{TOF}(K_i, d_j)}{\sigma_{ij}} \right\}^2 \quad (3)$$

where *offset* and distances  $d_j$  are free parameters of the minimization and  $\text{TOF}(K_i, d_j)$  is the expected time of flight accounting for the energy loss of particles in the first detector and in the air.<sup>11</sup>

### 2.3.3 | The self-calibration approach

A self-calibration method was developed to remove the systematic uncertainties and measure the absolute energy independently from any external energy reference. The new proposed approach relies on the relative displacements of S2, which are known with good accuracy from the grooves' distances. It allows calibrating the system in terms of the first considered distance between the sensors, which might still be affected by positioning errors, and the global time *offset* between the signals from the two detectors. The self-calibration procedure is performed by taking measurements of the mean time differences of coincident protons crossing the two sensors at specific locations of S2, using a few monoenergetic beams whose energy value is not

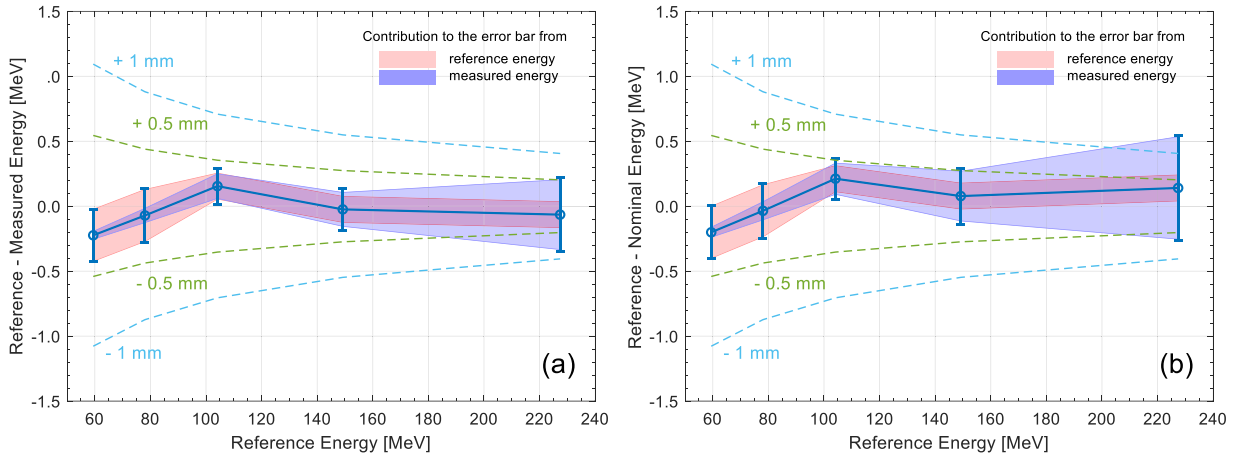


**FIGURE 3** Deviations between reference and measured energy for five different beam energies at the largest flight distance (97 cm) as a result of self- (a) and relative calibration (b). The blue and red shaded regions represent respectively, the errors on the measured and reference energies, while the error bars correspond to the uncertainty on the difference. The dot-lines show the corresponding deviations in the water range within 1 and 0.5 mm.

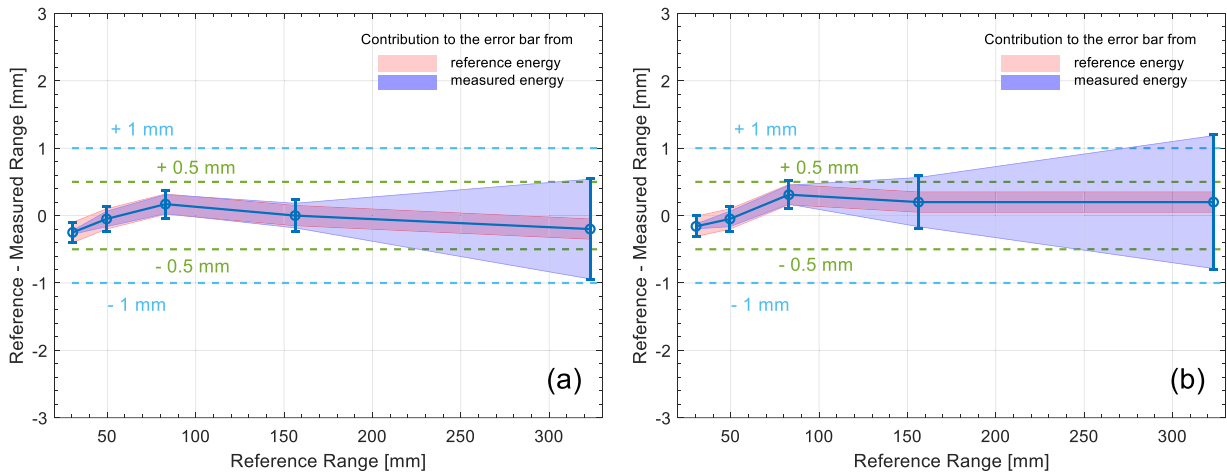


**FIGURE 4** Deviations between five reference and measured energies converted into a range 80% using the PSTAR dataset at the largest flight distance (97 cm) as a result of self- (a) and relative calibration (b).

used in the method. A minimization procedure aims at finding the estimated relative position of S2, for each S2 location and all the considered beams, in terms of the two unknown quantities.

A scheme of the basic principle is reported in Figure 2 and described in the following.

Depending on the number of grooves of the rigid horizontal support, several locations of the second sensor S2 might be set ( $p_1$ – $p_4$  in Figure 2). The relative displacements  $\Delta d_m$  between the S2 position  $p_m$  along the beam trajectory and the first S2 position  $p_1$ , are known from the grooves' distances with a very small uncertainty, while the distance  $x_0$  between S1 (fixed at  $p_0 = \text{isocenter}$ ) and the first S2 position ( $p_1$ ) is affected by a large uncertainty. Indeed,  $x_0$  depends on how the boards and the sensors are assembled, the sensor thickness, and any possible tilt of the different components.

By measuring the mean time difference of coincident signals  $\Delta t_{\text{mean}}$  for two different S2 locations (e.g.,  $p_2$  and  $p_3$  in step 1 of Figure 2) for the same beam energy, the average velocity of protons traveling across the distance  $d_{23}$  between  $p_2$  and  $p_3$  can be defined independently from  $x_0$  and *offset* as:

$$\begin{aligned}
 v_{\text{avg},23} &= \frac{d_{23}}{\text{TOF}_3 - \text{TOF}_2} \\
 &= \frac{p_3 - p_2}{(\Delta t_{\text{mean},3} - \text{offset}) - (\Delta t_{\text{mean},2} - \text{offset})} \\
 &= \frac{\Delta d_3 - \Delta d_2}{\Delta t_{\text{mean},3} - \Delta t_{\text{mean},2}} \quad (4)
 \end{aligned}$$

**TABLE 2** Self- (left column) and relative (right column) calibration parameters resulting from nine  $\Delta t_{mean}$  measurements (three energies and three distances) for the TPC beam test.

| Self        |        |       | Relative    |        |       |
|-------------|--------|-------|-------------|--------|-------|
| Parameter   | Value  | Error | Parameter   | Value  | Error |
| Offset (ps) | -90.1  | 1.5   | Offset (ps) | -95.7  | 3.1   |
| $x_0$ (cm)  | 26.932 | 0.025 | $d_1$ (cm)  | 27.031 | 0.047 |
|             |        |       | $d_2$ (cm)  | 66.939 | 0.052 |
|             |        |       | $d_3$ (cm)  | 97.045 | 0.052 |

and the average kinetic energy of protons traveling between  $p_2$  and  $p_3$  can be obtained from

$$K_{avg,23} = E_0 \left( 1 / \sqrt{1 - \left( \frac{v_{avg}}{c} \right)^2} - 1 \right) \quad (5)$$

as in step 2 of Figure 2.

The average kinetic energy in the distance  $d_{23}$ , corrected for the energy loss in the air,<sup>11</sup> is used to obtain the beam kinetic energy  $K_1$  at the exit of the first sensor S1 (step 3 in Figure 2), as a function of  $x_0$ .

From  $K_1$ , the mean velocity ( $v_{avg}$ ) between the two sensors for any S2 location can be determined (e.g.,  $v_{avg,p4}$  for S2 located in  $p_4$  as in step 4 of Figure 2), considering the appropriate energy loss in the air, and hence the S2 position (e.g.,  $p_4$ ) using the corresponding measured time difference  $\Delta t_{mean}$ . This *calculated* position, which depends on the values of  $x_0$  and *offset* parameters, is obtained using different combinations of S2 locations to evaluate  $v_{avg}$  and with all the beams considered. The whole process is then repeated for all the positions  $p_i$ .

The self-calibration aims at finding the  $x_0$  and *offset* parameters able to simultaneously minimize the square deviation between all the *calculated* and *measured* S2 positions, where the *measured* positions are those obtained by summing  $x_0$  to the specific  $\Delta d$  considered (step 5 in Figure 2).

## 2.4 | Beam tests at CNAO and TPC

The telescope systems with HPK pad sensors and FBK strip sensors (Figure 1) were tested, respectively, in a clinical treatment room of the CNAO facility,<sup>11</sup> and in the experimental room of the TPC.

At CNAO, only one out of the four pads has been readout for each sensor, and the ToF measurements were performed for five reference proton beam energies (59.4, 78.1, 104.1, 149.2, 227.4 MeV) retrieved from five distal water equivalent depths measured by CNAO using a Peakfinder (respectively R80: 30.4, 49.6, 82.9, 156.3, 323.2 mm),<sup>6</sup> at a beam flux of  $5 \times 10^8$  p s<sup>-1</sup> cm<sup>-2</sup>. For

each beam energy, the two sensors were positioned at four distances (7, 37, 67, 97 cm) from each other.

At TPC, only one strip has been readout for each detector, and the two sensors were positioned at three distances (27, 67, 97 cm). For each distance, the ToF measurements were performed at seven reference proton beam energies (68.5, 97.0, 147.1, 163.1, 182.8, 222.9, 227.4 MeV), corresponding to the distal water equivalent ranges at isocenter (respectively R90: 39, 73, 152, 182, 222, 312, 323 mm) measured by the facility with a Giraffe detector. The beam flux was adjusted for each energy in order to have a fluency of  $10^8$  p s<sup>-1</sup> cm<sup>-2</sup> approximately.

As described in our previous study,<sup>11</sup> the laser alignment system of both facilities was used to position S1 at the isocenter. Then, for each longitudinal distance, the transversal position of S2 was changed covering a grid using the movable stages. It was considered the best S2 alignment, the grid point providing the most significant number of coincidences.

After the alignment procedure, the mean time difference value was measured in a dedicated run for each reference beam energy and distance between the sensors. For each run, from 5000 to 15 000 waveforms were acquired from the digitizer, corresponding to a total acquisition time of around 3–9 s, respectively. Notably, the beam irradiation time was increased when increasing the distance to compensate for the loss of coincidence efficiency.

The beam energy was derived from the mean value of the time difference, performing the system calibration previously described, and then compared to the reference one, as described in the following.

## 3 | RESULTS

The self-calibration method was tested with the experimental data acquired at CNAO and TPC with clinical proton beams, and the results were compared with those previously obtained using the relative calibration approach.<sup>11</sup>

### 3.1 | CNAO

The system was calibrated using 16  $\Delta t_{mean}$  measurements performed at four beam energies (59.4, 78.1, 149.2, 227.4 MeV) and four distances (7, 37, 67, 97 cm). One proton beam energy (104.1 MeV) was not considered for the calibration procedure and was used as an independent test point. A statistical error on the measured  $\Delta t_{mean}$  in the order of a few ps was found. The output parameters (time *offset* and distances) resulting from the two calibration strategies are shown in Table 1.

A good correspondence is found between the *offset* parameters and the first distance ( $x_0$  and  $d_1$ ) between



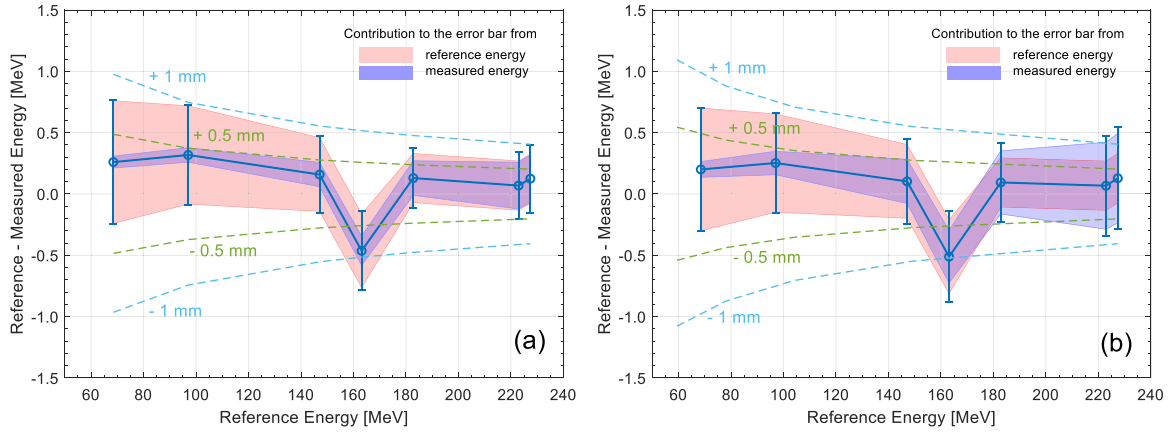


**FIGURE 5** Deviations between reference and measured energy for seven different beam energies at the largest flight distance (97 cm) as a result of the self-calibration (a) and the relative calibration (b). The blue and red shaded regions represent respectively, the errors on the measured and reference energies, while the error bars correspond to the uncertainty on the difference. The dot-lines show the corresponding deviations in the water range within 1 and 0.5 mm.

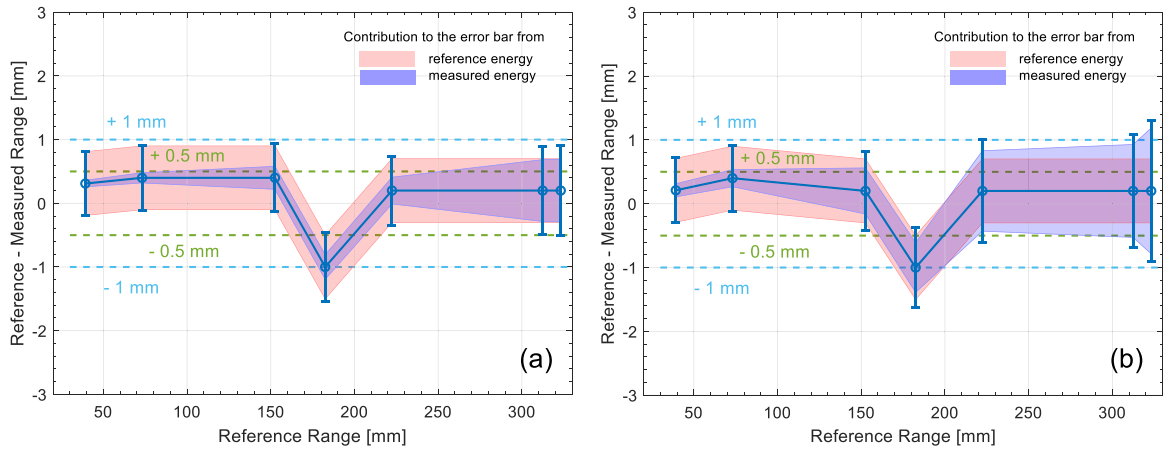


**FIGURE 6** Deviations between seven reference and measured energies converted into a range 80% using the PSTAR dataset at the largest flight distance (97 cm) as a result of self- (a) and relative calibration (b).

the two methods. However, the errors on the parameters resulting from the self-calibration approach are reduced by a factor 2 with respect to the relative method, thus allowing to achieve the required tolerance on the ToF measurement ( $\sim 3$  ps at 230 MeV and 1 m distance) for the two largest flight distances (67 and 97 cm).

The results regarding the deviation between reference and measured energy for the two calibration strategies are reported in Appendix 1 (Table A1.1), where the corresponding uncertainties were propagated from the error on  $\Delta t_{mean}$  and on calibration parameters.

As expected, the uncertainty on the measured energy decreases with decreasing beam energy and increasing the distance between sensors, since the requirements on the ToF measurement are less stringent, despite the loss of efficiency.

Figures 3 and 4 show the difference between reference and measured energies at the largest flight

distance (97 cm) in terms of energy and range for all the tested beam energies. The uncertainty on reference energies was derived from the corresponding range accuracy of 0.15 mm, measured in the CNAO treatment room with a Peakfinder water column. Both calibration methods led to a water range discrepancy below 0.5 mm. Notably, deviations in the order of a few hundreds of keV with a maximum uncertainty of 0.4 MeV on the measured energy were found as a result of the self-calibration approach, in compliance with the clinical requirements.

### 3.2 | TPC

At TPC, the system was calibrated using 9  $\Delta t_{mean}$  measurements performed at three energies (68.5, 182.8, 227.4 MeV) and three distances (27, 67, 97 cm), while all remaining acquired energies (97.0, 147.1, 163.1,

222.9 MeV) were used to test the results of the calibration independently. Table 2 reports the output parameters for the two calibration strategies. The results for the two largest flight distances (67 and 97 cm), which provide a more accurate energy measurement, are shown in Appendix 1 (Table A1.2). As already observed, the errors on the calibration parameters are reduced by nearly a factor 2 with the self-calibration approach.

Similarly to CNAO results, energy deviations from reference values of a few hundred keV were observed, in agreement with the clinical requirements. Notably, at 97 cm (Figures 5 and 6), most of the energy differences were found to lie within the water range tolerance of 0.5 mm with a level of uncertainty, that is, well below the one on the reference energies, which are estimated in the TPC experimental room with a range accuracy of 0.5 mm.

## 4 | DISCUSSION

The protons ToF measurement was demonstrated to be a promising approach for the energy assessment of clinical beams.<sup>11</sup> This work presents an upgraded version of the telescope device aimed at this scope, tested at two treatment centers (at CNAO—Pavia and TPC—Trento) with proton beams of clinical energies (59–227 MeV) and fluence rates (approximately  $10^8$  p/cm<sup>2</sup>·s), thus showing the capability to deal with different beam time structures resulting from both synchrotron and cyclotron accelerators.

Only one channel per sensor (either HPK pad sensors at CNAO or FBK strips at TPC) was bonded to the readout board, and a mechanical system consisting of a horizontal rigid support with 10 grooves was used to vary the distance between the sensors along the beam trajectory, with the first sensor S1 being kept fixed at the isocenter.

This study introduces a robust calibration method (self-calibration method) of the telescope device for the direct and absolute measurement of the energy of therapeutic proton beams. The procedure was developed to remove the systematic uncertainties due to the experimental setup (routing of the electronic chain and first distance between the sensors) independently from any a priori knowledge of the parameters of the monoenergetic beams used. This novel calibration method was successfully validated with simulated data and then benchmarked against a relative approach, which exploits the reference energy values provided by the facility, using the experimental data acquired at CNAO and TPC. For irradiation times of less than 10 s, uncertainties in the order of a few picoseconds on the measured time differences were observed. Furthermore, the self-calibration method allowed to halve the uncertainties on the system unknown parameters and to

obtain a few hundred keV deviations between reference and measured beam energies both at CNAO and TPC at the largest distance between the sensors (in compliance with the clinically required water range accuracy of 1 mm).

The impact of positioning uncertainties of the sensors was considered by evaluating the outcome on the energy measurement induced by variations in second sensor (S2) positions, thus simulating possible inaccuracies of the mechanical system. The self-calibration procedure was iteratively performed varying the relative displacements of S2 and the positioning accuracy in the order of a few hundreds of  $\mu$ m was necessary to keep the energy deviation below the clinical tolerance.

A sophisticated mechanical support is currently being developed to reduce the effect of systematic uncertainties related to the absolute distances between the sensors and to allow a 180° rotation of the system, useful to invert the order of the sensors along the beam and directly determine the time offset due to the routing of the electronic chain.

To reduce the statistical error on the measured time differences and improve the data acquisition system, a new front-end electronics board is being developed to simultaneously readout multiple strips per sensor, aiming to enlarge the sensitive area and to increase the number of coincident protons.

At present, the dead time of the data acquisition represents the main limitation of the system. Nevertheless, the data acquisition time required to achieve 1 mm range precision (a few tens of ms active acquisition and a few seconds total acquisition), together with the limited beam perturbation, make the telescope system a possible candidate for online monitoring of the beam energy and could find clinical application for fast beam commissioning and QA procedures. Moreover, the method can be easily applied to monitor the energy of clinical beams of heavier ions (e.g., carbon). Indeed, the clinical energy ranges correspond approximately to the same range of particle velocities of the present study and, consequently, lead to the same constraints on the ToF resolution to meet the clinical requirements. However, the sensors would need to be optimized for different particle species.

## 5 | CONCLUSIONS

The capability of a telescope detector made of two thin UFSD sensors to provide an absolute, direct, accurate, and fast measurement of the energy of clinical proton beams exploiting ToF assessment, independently from the beam temporal structure, has been demonstrated.

A dedicated self-calibration approach was developed to determine the system unknown parameters (absolute distance between the sensors and global time offset) independently from any external reference.

Improvements in the system are foreseen to find applications in beam commissioning, QA measurements, and online beam monitoring for all the present and future particles used for therapy.

## ACKNOWLEDGMENTS

This work was financed by the INFN CSN V, Ministero della Ricerca PRIN 2017 project “4DInsiDe” (MIUR PRIN 2017L2XKTJ). In addition, it has been supported by MIUR Dipartimenti di Eccellenza, Italy (ex L.232/2016, art.1, cc. 314, 337).

The authors kindly acknowledge the dedicated collaboration of Fondazione Bruno Kessler (FBK).

The content is object of Italian Patent Application No. 102021000025190 filed on 30.09.2021.

## CONFLICT OF INTEREST STATEMENT

The authors declare no conflicts of interest.

## REFERENCES

- Farr JB, Flanz JB, Gerbershagen A, Moyers MF. New horizons in particle therapy systems. *Med Phys*. 2018;45(11):e953-e983. doi:10.1002/mp.13193
- Riboldi M, Orecchia R, Baroni G. Real-time tumour tracking in particle therapy: technological developments and future perspectives. *Lancet Oncol*. 2012;13(9):383-391. doi:10.1016/S1470-2045(12)70243-7
- Giordanengo S, Palmans H. Dose detectors, sensors, and their applications. *Med Phys*. 2018;45(11):e1051-e1072. doi:10.1002/mp.13089
- Gilllin MT, Sahoo N, Bues M, et al. Commissioning of the discrete spot scanning proton beam delivery system at the University of Texas M.D. Anderson Cancer Center, Proton Therapy Center, Houston. *Med Phys*. 2010;37(1):154-163. doi:10.1118/1.3259742
- Giordanengo S, Manganaro L, Vignati A. Review of technologies and procedures of clinical dosimetry for scanned ion beam radiotherapy. *Physica Med*. 2017;43:79-99. doi:10.1016/j.ejmp.2017.10.013
- Mirandola A, Molinelli S, Freixas GV, et al. Dosimetric commissioning and quality assurance of scanned ion beams at the Italian National Center for Oncological Hadrontherapy. *Med Phys*. 2015;42(9):5287-5300. doi:10.1118/1.4928397
- Rana S, Bennouna J, Samuel EJJ, Gutierrez AN. Development and long-term stability of a comprehensive daily QA program for a modern pencil beam scanning (PBS) proton therapy delivery system. *J Appl Clin Med Phys*. 2019;20(4):29-44. doi:10.1002/ACM2.12556
- Sacchi R, Ganjeh ZA, Arcidiacono R, et al. Test of innovative silicon detectors for the monitoring of a therapeutic proton beam. *J Phys Conf Ser*. 2020;1662(12002). doi:10.1088/1742-6596/1662/1/012002
- Vignati A, Donetti M, Fausti F, et al. Thin low-gain avalanche detectors for particle therapy applications. *J Phys Conf Ser*. 2020;1662(1):012035. doi:10.1088/1742-6596/1662/1/012035
- Vignati A, Monaco V, Attili A, et al. Innovative thin silicon detectors for monitoring of therapeutic proton beams: preliminary beam tests. *J Instrum*. 2017;12(12):C12056-C12056. doi:10.1088/1748-0221/12/12/C12056
- Vignati A, Giordanengo S, Milian FM, et al. A new detector for the beam energy measurement in proton therapy: a feasibility study. *Phys Med Biol*. 2020;65(21). doi:10.1088/1361-6560/ABAB58
- Rabin NV. Status and possibilities of the time-of-flight measurement technique using long scintillation counters with a small cross section (Review. *Instrum Exp Tech*. 2007;50(5):579-638. doi:10.1134/S0020441207050016
- Krah N, Dauvergne D, Letang JM, Rit S, Testa E. Relative stopping power resolution in time-of-flight proton CT. *Phys Med Biol*. 2022;67(16):165004. doi:10.1088/1361-6560/AC7191
- Ulrich-Pur F, Bergauer T, Burkner A, et al. Feasibility study of a proton CT system based on 4D-tracking and residual energy determination via time-of-flight. *Phys Med Biol*. 2022;67(9). doi:10.1088/1361-6560/AC628B
- Worstell WA, Adams BW, Aviles M, et al. First results developing time-of-flight proton radiography for proton therapy applications. Proc. SPIE 10948, Medical Imaging 2019: Physics of Medical Imaging. 2019; 109480G. doi:10.1117/12.2511804
- Galizzi F, Caldara M, Jef A. A Time-of-Flight based energy measurement system for the LIGHT medical accelerator. *J Phys Conf Ser*. 2018;1067(7):072019. doi:10.1088/1742-6596/1067/7/072019
- Kormány Z. A new method and apparatus for measuring the mean energy of cyclotron beams. *Nucl Instrum Methods Phys Res A*. 1994;337(2-3):258-264. doi:10.1016/0168-9002(94)91093-6
- Milluzzo G, Scuderi V, Alejo A, et al. A new energy spectrum reconstruction method for time-of-flight diagnostics of high-energy laser-driven protons. *Rev Sci Instrum*. 2019;90(8):083303. doi:10.1063/1.5082746
- Tommasino F, Rovituso M, Fabiano S, et al. Proton beam characterization in the experimental room of the Trento Proton Therapy facility. *Nucl Instrum Methods Phys Res A*. 2017;869:15-20. doi:10.1016/J.NIMA.2017.06.017
- Marti Villarreal OA, Vignati A, Giordanengo S, et al. (2023). Characterization of thin LGAD sensors designed for beam monitoring in proton therapy. *Nucl Instrum Methods Phys Res A*. 2023;1046:167622. doi:10.1016/J.NIMA.2022.167622
- Sadrozinski HFW, Anker A, Chen J, et al. Ultra-fast silicon detectors (UFSD). *Nucl Instrum Methods Phys Res A*. 2016;831:18-23. doi:10.1016/J.NIMA.2016.03.093
- Pellegrini G, Fernández-Martínez P, Baselga M, et al. Technology developments and first measurements of Low Gain Avalanche Detectors (LGAD) for high energy physics applications. *Nucl Instrum Methods Phys Res A*. 2014;765:12-16. doi:10.1016/J.NIMA.2014.06.008
- Cartiglia N, Staiano A, Sola V, et al. Beam test results of a 16 ps timing system based on ultra-fast silicon detectors. *Nucl Instrum Methods Phys Res A*. 2017;850:83-88. doi:10.1016/J.NIMA.2017.01.021

**How to cite this article:** Vignati A, Mas Milian FM, Shakarami Z, et al. Calibration method and performance of a time-of-flight detector to measure absolute beam energy in proton therapy. *Med Phys*. 2023;1-11. <https://doi.org/10.1002/mp.16637>

## APPENDIX A

**TABLE A1.1** List of the measured ToFs and energies at the isocenter for the two largest flight distances (67 and 97 cm) with the corresponding deviation and uncertainties according to the relative and self-calibration approach for the CNAO beam test.

| Distance (cm) |          | $E_{\text{ref}}$ (MeV) | $\sigma_{E_{\text{ref}}}$ (MeV) | ToF (ns) |          | $\sigma_{\text{ToF}}$ (ns) |          | $E_{\text{meas}}$ (MeV) |          | $\sigma_{E_{\text{meas}}}$ (MeV) |          | $E_{\text{ref}} - E_{\text{meas}}$ (MeV) |          | $\sigma_{\text{Dev}}$ (MeV) |          |
|---------------|----------|------------------------|---------------------------------|----------|----------|----------------------------|----------|-------------------------|----------|----------------------------------|----------|--|----------|-----------------------------|----------|
| Self          | Relative |                        |                                 | Self     | Relative | Self                       | Relative | Self                    | Relative | Self                             | Relative | Self                                     | Relative | Self                        | Relative |
| 66.605        | 66.663   | 227.4                  | 0.1                             | 3.746    | 3.748    | 0.002                      | 0.004    | 227.7                   | 227.6    | 0.4                              | 0.6      | -0.3                                     | -0.2     | 0.4                         | 0.6      |
|               |          | 149.2                  | 0.1                             | 4.404    | 4.405    | 0.002                      | 0.004    | 149.1                   | 149.1    | 0.2                              | 0.3      | 0.1                                      | 0.1      | 0.2                         | 0.3      |
|               |          | 104.1                  | 0.1                             | 5.114    | 5.116    | 0.002                      | 0.004    | 104.2                   | 104.1    | 0.1                              | 0.1      | -0.05                                    | -0.01    | 0.1                         | 0.2      |
|               |          | 78.1                   | 0.2                             | 5.805    | 5.807    | 0.002                      | 0.004    | 78.1                    | 78.1     | 0.1                              | 0.1      | -0.1                                     | -0.1     | 0.2                         | 0.2      |
|               |          | 59.4                   | 0.2                             | 6.582    | 6.584    | 0.003                      | 0.004    | 59.4                    | 59.4     | 0.04                             | 0.06     | 0.001                                    | 0.008    | 0.2                         | 0.2      |
| 96.605        | 96.727   | 227.4                  | 0.1                             | 5.440    | 5.442    | 0.002                      | 0.004    | 227.5                   | 227.3    | 0.3                              | 0.4      | -0.1                                     | 0.1      | 0.3                         | 0.4      |
|               |          | 149.2                  | 0.1                             | 6.391    | 6.392    | 0.002                      | 0.004    | 149.2                   | 149.1    | 0.1                              | 0.2      | -0.02                                    | 0.08     | 0.2                         | 0.2      |
|               |          | 104.1                  | 0.1                             | 7.431    | 7.433    | 0.003                      | 0.004    | 104.0                   | 103.9    | 0.1                              | 0.1      | 0.2                                      | 0.2      | 0.1                         | 0.2      |
|               |          | 78.1                   | 0.2                             | 8.432    | 8.434    | 0.003                      | 0.004    | 78.1                    | 78.1     | 0.1                              | 0.1      | -0.1                                     | 0.01     | 0.2                         | 0.2      |
|               |          | 59.4                   | 0.2                             | 9.549    | 9.551    | 0.003                      | 0.004    | 59.7                    | 59.6     | 0.03                             | 0.04     | -0.2                                     | -0.2     | 0.2                         | 0.2      |

**TABLE A1.2** List of the measured ToFs and energies at the isocenter for the two largest flight distances (67 and 97 cm) with the corresponding deviations and uncertainties according to the relative and self-calibration approach for the Trento beam test.

| Distance (cm) |          | $E_{\text{ref}}$ (MeV) | $\sigma_{E_{\text{ref}}}$ (MeV) | ToF (ns) |          | $\sigma_{\text{ToF}}$ |          | $E_{\text{meas}}$ (MeV) |          | $\sigma_{E_{\text{meas}}}$ (MeV) |          | $E_{\text{ref}} - E_{\text{meas}}$ (MeV) |          | $\sigma_{\text{Dev}}$ (MeV) |          |
|---------------|----------|------------------------|---------------------------------|----------|----------|-----------------------|----------|-------------------------|----------|----------------------------------|----------|--|----------|-----------------------------|----------|
| Self          | Relative |                        |                                 | Self     | Relative | Self                  | Relative | Self                    | Relative | Self                             | Relative | Self                                     | Relative | Self                        | Relative |
| 66.932        | 66.939   | 227.4                  | 0.2                             | 3.754    | 3.76     | 0.002                 | 0.003    | 228.1                   | 228.2    | 0.3                              | 0.5      | -0.7                                     | -0.8     | 0.5                         | 0.5      |
|               |          | 222.9                  | 0.2                             | 3.785    | 3.791    | 0.002                 | 0.003    | 223.0                   | 223.0    | 0.3                              | 0.5      | -0.1                                     | -0.1     | 0.5                         | 0.4      |
|               |          | 182.8                  | 0.2                             | 4.082    | 4.088    | 0.002                 | 0.003    | 182.1                   | 182.1    | 0.2                              | 0.4      | 0.7                                      | 0.7      | 0.5                         | 0.4      |
|               |          | 163.1                  | 0.3                             | 4.263    | 4.269    | 0.002                 | 0.003    | 162.8                   | 162.9    | 0.2                              | 0.3      | 0.3                                      | 0.2      | 0.5                         | 0.4      |
|               |          | 97                     | 0.4                             | 5.298    | 5.304    | 0.002                 | 0.003    | 96.4                    | 96.5     | 0.08                             | 0.1      | 0.6                                      | 0.5      | 0.7                         | 0.5      |
|               |          | 68.5                   | 0.5                             | 6.184    | 6.190    | 0.002                 | 0.004    | 68.1                    | 68.2     | 0.05                             | 0.1      | 0.4                                      | 0.3      | 1                           | 0.6      |
| 96.932        | 97.045   | 227.4                  | 0.2                             | 5.453    | 5.459    | 0.002                 | 0.003    | 227.3                   | 227.3    | 0.2                              | 0.4      | 0.1                                      | 0.1      | 0.4                         | 0.4      |
|               |          | 222.9                  | 0.2                             | 5.492    | 5.498    | 0.002                 | 0.003    | 222.8                   | 222.8    | 0.2                              | 0.3      | 0.1                                      | 0.1      | 0.4                         | 0.4      |
|               |          | 182.8                  | 0.2                             | 5.914    | 5.920    | 0.002                 | 0.003    | 182.7                   | 182.7    | 0.1                              | 0.3      | 0.1                                      | 0.1      | 0.5                         | 0.3      |
|               |          | 163.1                  | 0.3                             | 6.173    | 6.179    | 0.002                 | 0.003    | 163.6                   | 163.6    | 0.1                              | 0.2      | -0.5                                     | -0.5     | 0.5                         | 0.4      |
|               |          | 147.1                  | 0.3                             | 6.442    | 6.448    | 0.002                 | 0.003    | 146.9                   | 147.0    | 0.1                              | 0.2      | 0.2                                      | 0.1      | 0.6                         | 0.3      |
|               |          | 97                     | 0.4                             | 7.679    | 7.685    | 0.002                 | 0.003    | 96.7                    | 96.7     | 0.06                             | 0.1      | 0.3                                      | 0.3      | 0.7                         | 0.4      |
|               |          | 68.5                   | 0.5                             | 8.972    | 8.978    | 0.003                 | 0.004    | 68.2                    | 68.3     | 0.05                             | 0.1      | 0.3                                      | 0.2      | 1                           | 0.5      |